A NUMERICAL STUDY ON HEAT TRANSFER FOR MHD FLOW OF RADIATIVE CASSON NANOFLUID OVER A POROUS STRETCHING SHEET

S. RAO and P.N. DEKA

Dibrugarh University, Dibrugarh, Assam, 786004, India
shivarao374@gmail.com, pndeka@dibru.ac.in

***Abstract*— The current study deals with the heat transfer of the steady two-dimensional MHD Casson nanofluid flow over a non-linearly stretched porous sheet associated with viscous dissipation, chemical radiate parameters and thermal radiation. Using the appropriate similarity transformation, the non-linear partial differential equations are transformed into a system of coupled non-linear ordinary differential equations which are further numerically solved using a MATLAB built-in solver bvp4c (Boundary value problem of fourth-order). The comparison reveals an excellent agreement which proves the validation of the numerical approach. The effect of various MHD parameters on the velocity, temperature and nanoparticle concentration are discussed graphically whereas its impact on heat and mass transfer rate are shown in tabular form as Nusselt number and Sherwood number respectively. Enhancement in temperature profile is observed as a result of the increased value of the radiation parameter and Brownian motion parameter. In this study, both Newtonian and non-Newtonian cases are studied separately for each parameter. Moreover, this study demonstrates, when a porous sheet is stretched non-linearly under chemical and thermal radiation, the Casson nanofluid controls the temperature and nanoparticle concentration better than the Newtonian nanofluid.**

***Keywords*— Non-Newtonian, Casson nanofluid, Porous stretching sheet, Viscous dissipation, Chemical radiate, Steady flow.**

I. INTRODUCTION

Thermal capabilities of engineering industrial processes mainly revolve around the heat transfer quality of the fluid. The ability of heat transfer is increased by the increase in thermal conductivity. Convectional fluids have very low thermal conductivity, as a result, it cannot be used for ultra-high cooling processes. As a result of their high thermal conductivity, nanofluids are used in place of base fluids as working fluids these days. Choi (1995) was the first researcher to discover that the suspended nanoparticles in the base fluid could enhance the thermal conductivity. Lee *et al.* (1999) examined the thermal conductivity of several metal oxides and discovered that shape and size both played major roles in increasing the thermal conductivity of the nanofluid. Wang *et al.* (1999) explored the viscosity of Al2O3-water and CuO-water and found that 3% volume concentration of Al2O3-water nanofluid enhanced thermal conductivity up to 30%. Eastman *et al.* (2001) by their study conclude that the addition of copper nanoparticles with less than 1% volume fraction in ethylene glycol could increase the thermal conductivity up to 40%. Later on, many investigators (Xuan and Li, 2003) had revealed that by adding 1-5% of nanoparticles in the base fluid could enhance more than 20% of thermal conductivity. Buongiorno (2006) sought to explain the rise in the thermal conductivity of the nanofluid by pointing out two slip mechanisms i.e., Brownian motion of the particles and thermophoresis for effective enhancement of thermal conductivity of the base fluid. Nield and Kuznetsov, (2009) discussed the influence of Brownian motion and thermophoresis on a horizontal boundary layer of porous medium saturated by a nanofluid. Khan and Pop (2010) explored the problem of steady two-dimensional laminar fluid flow of a nanofluid over a stretching flat plate. Different scholars investigated the nanofluid flow on different model and presented some notable results, as some of them in reference (Rana *et al.*, 2012; Makinde *et al.*, 2018)

Pandey and Kumar (2017), studied the flow of Cu-water nanofluid over a porous stretching cylinder under thermal radiation, viscous dissipation and slip conditions. Joshi *et al.* (2021) investigated the heat and mass transfer of hybrid nanofluid over a bidirectional porous stretching sheet under the effect of chemical reaction and heat generation. Singh *et al.* (2021) made a numerical investigation to study the flow of micropolar nanofluid over a stretchable surface under chemical reaction and heat absorption/generation. Upreti *et al.* (2021) also used a numerical approach to study about the heat transfer of Sisko nanofluid over a stretchable Darcy – Forcheimer porous medium under thermal radiation. Very recently Upreti *et al.* (2020) and Pandey and Upreti (2021) have investigated heat transfer efficiency of nanofluids.

Non-Newtonian fluid is widely used in many industrial and technological sector, such as paint, glues, dissolved polymers, asphalts and biological solutions. Non-Newtonian fluids does not comply with Newton's law of viscosity i.e., where shear stress is not directly proportional to the gradient of velocity. For e.g.- Juice of apple, blood, honey, fluid, oils, cream, toothpaste, etc. Hady *et al.* (2011) and Cheng (2012) analyzed the non-Newtonian nanofluid over a porous vertical plate and porous vertical truncated cone. The natural convection of non-Newtonian nanofluid along a preamble cone which was vertical was analysed by Rashad *et al.* (2011). Mabood *et al.* (2015) explored the heat and mass transfer of MHD

nanofluid flow over a non-linear stretching sheet associated with viscous dissipation. Zaib *et al.* (2018) have discussed the Jeffery nanofluid over stretching sheet in details. Some advancements in non-Newtonian nanofluid are given in references (Hayat *et al.*, 2015; Raju *et al.*, 2016; Ramzan *et al.*, 2016).

Casson fluid is categorized as a non-Newtonian fluid. Tomato sauce, honey, soup, human blood, and orange juice are all examples of Casson fluid. The MHD Casson fluid over an unsteady stretched porous sheet with a chemical reaction was numerically investigated Makanda *et al.* (1999). Mustafa *et al.* (2011) studied the unsteady flow of a Casson fluid over a moving flat plate. Nandy (2013) studied the flow and heat transfer in a Casson non-Newtonian fluid over a stretching surface under slip condition. Nadeem *et al.* (2014) studied the two-dimensional steady flow and analyzed the convective boundary condition of Casson nanofluid. Malik *et al.* (2015) investigate a new kind of heat flux model on Casson nanofluid. Ibrahim *et al.* (2017) studied the effect of chemical reaction and heat source on dissipative MHD flow of Casson nanofluid over stretching sheet using H.A.M. approach for solving differential equations. They have investigated impacts of Casson parameter, suction parameter in improving heat and mass transfer rates. Shashikumar *et al.* (2017) investigated the radiation effect on Casson nanofluid between vertical plate. Rafique *et al.* (2019) made a numerical study to understand the impact of Soret and Dufour effect on nanofluid flow over a non-linear inclined surface. Lund *et al.* (2020) made a stability analysis on MHD Casson nanofluid through an exponentially stretching/shrinking sheet. Abdal *et al.* (2021) examined the Casson nanofluid flow under magnetic field over an extending cylinder. Recently much advances have been made on the investigation of the peristaltic motion of the Casson fluid. Some notable work can be seen in the refs. Manjunatha *et al.* (2019), Prasad *et al.* (2020) and Divya *et al.* (2021). Some recent advancement on Casson nanofluid are mentioned in the references by Abo-Dahab *et al.*, 2021; Zhou *et al.*, 2021; and Jamshed *et al.*, 2021.

The main aim of this present study is to scrutinize the Casson nanofluid under the effect of transverse magnetic field, radiation, chemical reaction, viscous dissipation over a porous nonlinear stretching sheet. This study also covers the comparison of both Newtonian and non-Newtonian nanofluid on its performance for efficiency in terms of all relevant parameters. Using an appropriate similarity transformation, the governing partial differential equations are transformed to ordinary differential equations and are numerically solved by MATLAB built-in solver bvp4c. To prove the validity of the numerical approach the current results are compared with the previous studies under some limiting cases. It is worth noting that the results are in perfect accord. This exploration may find its application in metallurgy, blood rheology and food processing.

II. MATHEMATICAL FORMULATION

Let us consider a viscous Casson nanofluid on a porous non-linearly stretching sheet. Both the sheet and the fluid are initially at rest. Stretching the sheet along the x-direction leads the fluid to start flowing uniformly at $y = 0$ with velocity $u_w = ax^n$, where $a > 0$; $n > 0$ are constants. The fluid is electrically conducting due to the magnetic field of the form $B = B_0 x^{\frac{n-1}{2}}$ normal to the x-axis with constant B_0. Here we consider a very low magnetic Reynolds number which results in a negligible induced magnetic field and no electric field. The wall temperature $T_w = T_\infty + Ax^n$ and concentration C_w at stretching sheet is considered to be constant. At $y \to \infty$ the ambient temperature T_∞ and ambient nanoparticle volume fraction C_∞ are assumed to be lesser than the temperature T_w and nanoparticle concentration C_w at the wall.

The rheological equations of Casson fluid for an incompressible and isotropic flow is given by (see refs. Mukhopadhyay *et al.*, 2013; Oyelakin *et al.*, 2016) –

$$\tau_{ij} = \begin{cases} \left(\mu_B + \frac{p_y}{\sqrt{2\pi}}\right) 2e_{ij}, & \pi < \pi_c \\ \left(\mu_B + \frac{p_y}{\sqrt{2\pi_c}}\right) 2e_{ij}, & \pi < \pi_c \end{cases} \quad (1)$$

where e_{ij} is the rate of strain tensor, μ_B is the Casson coefficient of viscosity, p_y is the yield stress of the fluid, $\pi = e_{ij}e_{ij}$ and π_c is the critical value of of the product in these Casson model.

The governing equations (see refs. Pai, 1956; Schichting, 1964; Kuznetsov and Nield, 2010) of the flow model is

$$\frac{\partial u}{\partial x} + \frac{\partial v}{\partial y} = 0 \quad (2)$$

$$u\frac{\partial u}{\partial x} + v\frac{\partial u}{\partial y} = \nu\left(1 + \frac{1}{\beta}\right)\frac{\partial^2 u}{\partial y^2} - \frac{\sigma_e B^2}{\rho}u - \frac{\nu}{k_0}u \quad (3)$$

$$u\frac{\partial T}{\partial x} + v\frac{\partial T}{\partial y} = \alpha\frac{\partial^2 T}{\partial y^2} + \frac{\nu}{C_p}\left(1 + \frac{1}{\beta}\right)\left(\frac{\partial u}{\partial y}\right)^2 + \tau\left(D_B\frac{\partial C}{\partial y}\frac{\partial T}{\partial y} + \frac{D_T}{T_\infty}\left(\frac{\partial T}{\partial y}\right)^2\right) - \frac{1}{\rho C_P}\frac{\partial q_r}{\partial y} \quad (4)$$

$$u\frac{\partial C}{\partial x} + v\frac{\partial C}{\partial y} = D_B\frac{\partial^2 C}{\partial y^2} + \frac{D_T}{T_\infty}\frac{\partial^2 T}{\partial y^2} - K_r(C - C_\infty) \quad (5)$$

where u and v are the velocity along x-axis and y-axis respectively $\nu = \frac{\mu}{\rho}$ is the kinetic viscosity (μ is the dynamic viscosity and ρ is the density) of the fluid, $\tau = \frac{(\rho C)_p}{(\rho C)_f}$ is the ratio between the effective heat capacity of nanoparticles and the effective heat capacity of base fluid, $\beta = \frac{\mu_B\sqrt{2\pi_c}}{p_y}$ is the Casson parameter, σ_e is the electrical conductivity, k_0 is the permeability of porous medium, $\alpha = \frac{\kappa}{\rho C_p}$ is the thermal diffusivity (κ is the thermal conductivity and C_p is the specific heat), D_B and D_T are coefficient of Brownian and thermophoretic diffusion parameter respectively and K_r is the reaction coefficient.

The boundary condition (see refs. Khan and Pop, 2010) in the present problem are-

$$\text{At } y = 0: \quad u_w = ax^n, \quad v = 0,, \quad T = T_w = T_\infty + T_0x^n, \quad C = C_w$$

Table 1: Comparison of numerical values when Pr =Le=2, Nb = 0.5, M=E_c=K= R_d=γ = 0 and $\beta = \infty$

n	Nt	Rana and Bhargava, (2012)		Mabood *et al.*, (2015)		Present study	
		$-\theta'(0)$	$-\phi'(0)$	$-\theta'(0)$	$-\phi'(0)$	$-\theta'(0)$	$-\phi'(0)$
	0.1	0.5160	0.9012	0.5148	0.9014	0.5144	0.9009
0.2	0.3	0.4533	0.8395	0.4520	0.8402	0.4517	0.8400
	0.5	0.3999	0.8048	0.3987	0.8059	0.3983	0.8063
	0.1	0.4864	0.8445	0.4852	0.8447	0.4849	0.8448
3.0	0.3	0.4282	0.7785	0.4271	0.7791	0.4266	0.7802
	0.5	0.3786	0.7379	0.3775	0.7390	0.3767	0.7418
	0.1	0.4799	0.8323	0.4788	0.8325	0.4785	0.8327
10.0	0.3	0.4227	0.7654	0.4216	0.7660	0.4211	0.7675
	0.5	0.3739	0.7238	0.3728	0.7248	0.3719	0.7284

$$\mathrm{y} \to \infty: \quad u = 0, \quad \mathrm{v} = 0, \qquad \mathrm{T} = \mathrm{T}_\infty, \quad \mathrm{C} = \mathrm{C}_\infty \quad (6)$$

The Rosseland approximation for radiative heat flux can be mathematically written as (see refs. Brewster, 1972; Sparrow and Cess, 1978; Raptis, 1998)

$$\mathrm{q_r} = \frac{-4\sigma^*}{3\mathrm{k}^*}\frac{\partial \mathrm{T}^4}{\partial \mathrm{y}} \quad (7)$$

where σ^* and k^* are Stefan-Boltzmann and mean absorption coefficient respectively.

Expanding the Taylor series and neglecting the higher order, we get

$$\mathrm{T}^4 = 4\,\mathrm{T}_\infty^3\,\mathrm{T} - 3\,\mathrm{T}_\infty^4$$

Hence eq. (7) becomes-

$$\frac{\partial \mathrm{q_r}}{\partial \mathrm{y}} = \frac{-16\sigma^*}{3\mathrm{k}^*}\,\mathrm{T}_\infty^3\frac{\partial^2 \mathrm{T}}{\partial \mathrm{y}^2} \quad (8)$$

The similarity transformation to make Eqns. (2) to (5) dimensionless are (Rana and Bhargava, 2012)

$$\eta = \mathrm{y}\sqrt{\frac{\mathrm{a(n+1)}}{2\nu}}\mathrm{x}^{(\mathrm{n}-1)/2},\ u = \mathrm{ax^n f'}(\eta),$$
$$\mathrm{v} = -\sqrt{\frac{\mathrm{a}\nu(\mathrm{n}+1)}{2}}\mathrm{x}^{(\mathrm{n}-1)/2}\left(\mathrm{f}(\eta) + \frac{\mathrm{n}-1}{\mathrm{n}+1}\eta\mathrm{f}'(\eta)\right), \quad (9)$$
$$\theta(\eta) = \frac{\mathrm{T}-\mathrm{T}_\infty}{\mathrm{T_w}-\mathrm{T}_\infty},\ \phi(\eta) = \frac{\mathrm{C}-\mathrm{C}_\infty}{\mathrm{C_w}-\mathrm{C}_\infty}$$

Equations (3) to (5) with the help of Eq. (9) are transformed to the non-linear ODE's

$$\left(1+\frac{1}{\beta}\right)\mathrm{f'''} + \mathrm{ff''} - \left(\frac{2\mathrm{n}}{\mathrm{n}+1}\right)\mathrm{f'^2} - (M+K)\mathrm{f'} = 0 \quad (10)$$

$$\frac{1}{Pr}(1+Rd)\theta'' + \mathrm{f}\theta' + Nb\phi'\theta' + Nt\theta'^2 + Ec\left(1+\frac{1}{\beta}\right)\mathrm{f''}^2 = 0 \quad (11)$$

$$Le\,\mathrm{f}\,\phi' + \frac{Nt}{Nb}\theta'' - \gamma\,Le\,\phi = 0 \quad (12)$$

where $M = \frac{2\sigma_e B_0^2}{\mathrm{a}\rho(\mathrm{n}+1)}$ is the Magnetic parameter, $Pr = \frac{\nu}{\alpha}$is the Prandtl number, $Nb = \frac{(\rho\mathrm{C})_\mathrm{p}\mathrm{D_B}(\mathrm{C_w}-\mathrm{C}_\infty)}{(\rho\mathrm{C})_f}$ is the Brownian motion parameter, $Nt = \frac{(\rho\mathrm{C})_\mathrm{p}\mathrm{D_T}(\mathrm{T_W}-\mathrm{T}_\infty)}{(\rho\mathrm{C})_\mathrm{f}\mathrm{T}_\infty\nu}$ is Thermophoresis parameter, $Rd = \frac{16T_\infty^3\sigma^*}{3\kappa k^*}$is the radiation parameter, $Ec = \frac{u_w^2}{C_p(T_w-T_\infty)}$ is the Eckert number, $K = \frac{2\nu}{\mathrm{ak_0(n+1)}}\mathrm{x}^{-(\mathrm{n}-1)}$is the Permeability parameter , $Le = \frac{\nu}{\mathrm{D_B}}$ is the Lewis number and $\gamma = \frac{2\,\mathrm{K_r}}{\mathrm{a(n+1)}}\mathrm{x}^{-(\mathrm{n}-1)}$ is the Chemical reaction parameter.

The boundary condition from Eq. (6) in dimensionless form are as follows:

$$\mathrm{f}(0) = 0, \quad \mathrm{f'}(0) = 1, \quad \theta(0) = 1, \quad \phi(0) = 1$$
$$\mathrm{f'}(\infty) = 0, \quad \theta(\infty) = 0, \quad \phi(\infty) = 0 \quad (13)$$

The local skin friction coefficient, local nusselt number and local Sherwood number are defined as -

$$\mathrm{C_f} = \frac{\tau_\mathrm{w}}{\rho\mathrm{u}_w^2(\mathrm{x})}, \mathrm{Nu_x} = \frac{\mathrm{xq}_w}{\mathrm{k}(\mathrm{T}_w - \mathrm{T}_\infty)}, \mathrm{Sh_x} = \frac{\mathrm{xq_m}}{\mathrm{D_B}(\mathrm{C}_w - \mathrm{C}_\infty)}$$

where τ_w, q_w and q_m are the shear stress along stretching sheet, surface heat flux and mass flux respectively. These are mathematically expressed by-

$$\tau_\mathrm{w} = \mu_\mathrm{B}\left(1+\frac{1}{\beta}\right)\left(\frac{\partial \mathrm{u}}{\partial \mathrm{y}}\right)_{\mathrm{y}=0}, \quad \mathrm{q_w} = -\left(\frac{\partial \mathrm{T}}{\partial \mathrm{y}}\right)_{\mathrm{y}=0}$$
$$\text{and } q_m = -D_B\left(\frac{\partial C}{\partial y}\right)_{y=0}$$

III. METHOD OF SOLUTION

Equations (10) to (12) along with the boundary condition (13) are solved by using a MATLAB build-in solver called bvp4c. Eqn (10) to (12) are converted into the set of first order differential equations as follows:

$$\mathrm{f} = \mathrm{y}_1,\ \mathrm{f'} = \mathrm{y}_1' = \mathrm{y}_2,\ \mathrm{f''} = \mathrm{y}_2' = \mathrm{y}_3,\ \theta = \mathrm{y}_4,$$
$$\theta' = \mathrm{y}_4' = \mathrm{y}_5,\ \phi = \mathrm{y}_6,\ \phi' = \mathrm{y}_6' = \mathrm{y}_7,$$
$$\mathrm{f'''} = \frac{-\mathrm{y}_1\mathrm{y}_3 + \left(\frac{2\mathrm{n}}{\mathrm{n}+1}\right)\mathrm{y}_2{}^2 + (\mathrm{M}+\mathrm{K})\mathrm{y}_2}{\left(1+\frac{1}{\beta}\right)},$$
$$\theta'' = \frac{\mathrm{Pr}\left[-\mathrm{y}_1\mathrm{y}_5 - \mathrm{Nby}_7\mathrm{y}_5 - \mathrm{Nty}_5{}^2 - \mathrm{Ec}\left(1+\frac{1}{\beta}\right)\mathrm{y}_3{}^2\right]}{1+\mathrm{Rd}},$$
$$\phi'' = -Le\mathrm{y}_1\mathrm{y}_7 - \frac{Nt}{Nb}\theta'' + \gamma\mathrm{Ley}_6.$$

The boundary conditions are given as

$$y_1(0) = 0,\ y_2(0) = 1,\ y_4(0) = 1,\ y_6(0) = 1$$
$$y_2(\infty) = 1,\ y_4(\infty) = 0,\ y_6(\infty) = 0.$$

IV. RESULTS AND DISCUSSION

Here the influence of dimensionless parameter like Casson parameter (β), Thermophoresis parameter (Nt), chemical reaction parameter (γ), permeability parameter (K), Lewis number (Le), magnetic field parameter (M), Prandtl number (Pr) and Brownian motion parameter (Nb) on velocity profile, temperature profile, nanoparticle concentration profile, local Nusselt number and local Sherwood number are displayed using graphs and in tabular form.

In an attempt to check the authenticity of the results obtained a comparison is made with those of previous reported results of Rana and Bhargava (2012) and Mabood *et al.* (2015). Table (1) seems to be in excellent compliance and higher accuracy. In the same way Fig. 1 shows the authenticity of the scheme used.

Figures (2) to (15) shows the effect of different parameter on velocity profile, temperature profile and nanoparticle concentration for both Newtonian and non-

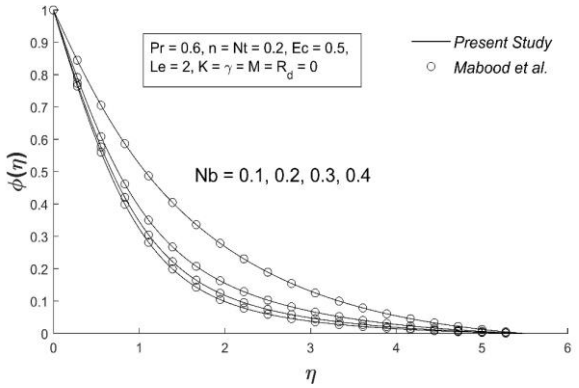

Figure 1: Comparison between Runge–Kutta–Fehlberg fourth fifth order method (Mabood *et al.*) and Matlab's Bvp4c Scheme (Present Study)

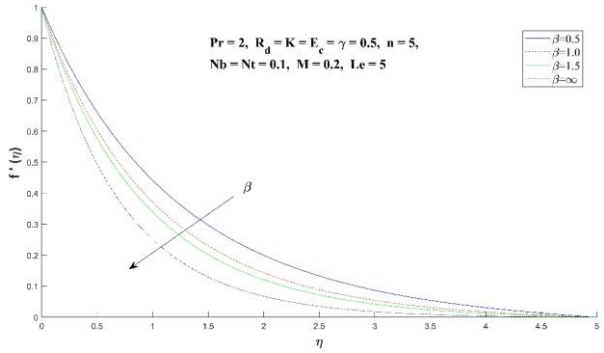

Figure 2: Influence of β on velocity profile

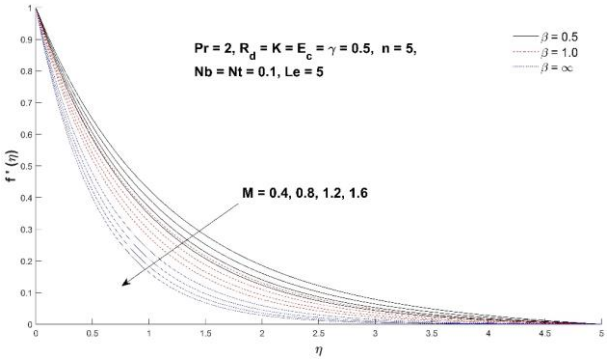

Figure 3: Influence of M on velocity profile for different values of β

Newtonian nanofluid with a significance of β = 0.5, 1.0 and ∞. This provides a comparative analysis on the impact of the variation of this parameter in case of both Newtonian and non-Newtonian.

Figure (2) displays the effect of Casson parameter on velocity profile. It can be observed that the increase of Casson parameter reduces the velocity. This is due to the fact that increase in Casson parameter leads to enhancement of fluid viscosity which eventually resist the fluid flow in x-direction. It is interesting to note that the current problem transforms to Newtonian nanofluid case when $\beta \to \infty$.

Figure (3) and (4) exhibits the variation in velocity and temperature profile for different values of M long with β. Here, it is shown that the increasing magnetic parameter leads to a reduction in velocity profile but increasing behavior in temperature profile. As the magnetic

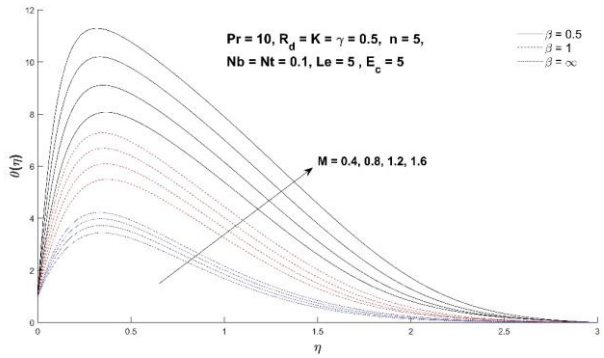

Figure 4: Effect of M on temperature profile for different values of β

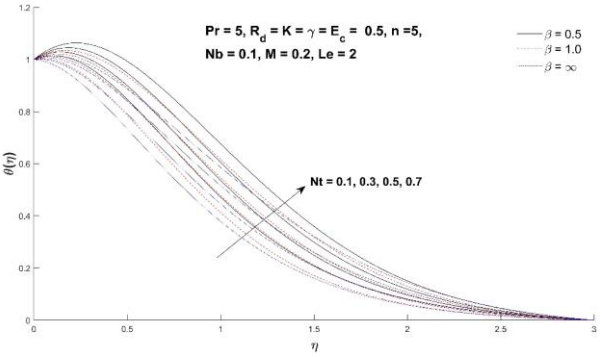

Figure 5: Influence of Nt on temperature profile for different values of β

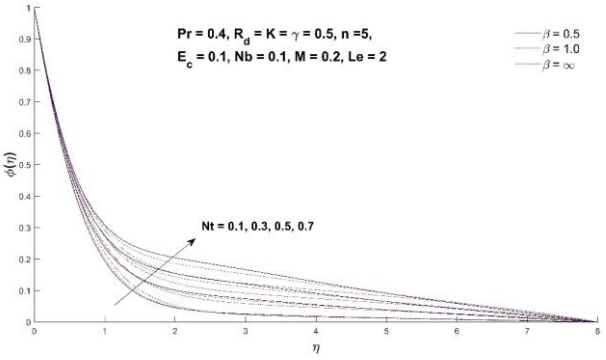

Figure 6: Influence of Nt on nanoparticle concentration for different values of β

field parameter increases, a resistive force called a Lorentz force is produced which retards in the form magnetic pressure drop on the velocity, as a result the motion gets slowed down. Therefore, the velocity decreases with the increasing value of M. Again due to the Lorentz force a resistance is offered to the flow which results in warming up the boundary layer region. Hence the temperature increases as the values of M gets increase.

Figures (5) and (6) depicts that the increase in Nt leads to the increase in both temperature and nanoparticle concentration profile. The reason behind the fact is that the increase in Nt results the enhancement of thermophoresis forces which has the tendency to fast flow the nanoparticles from hot surface to cold surface away from stretching. This results in an increase of heat and mass transfer in the boundary layer region for nanoparticles.

Figures (7) and (8) reveals the influence of Nb on temperature and nanoparticle concentration respectively for different cases of β. It is evident from the figure that

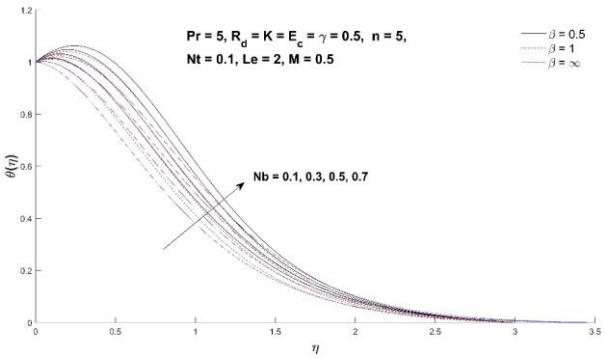

Figure 7: Influence of Nb on temperature profile for different values of β

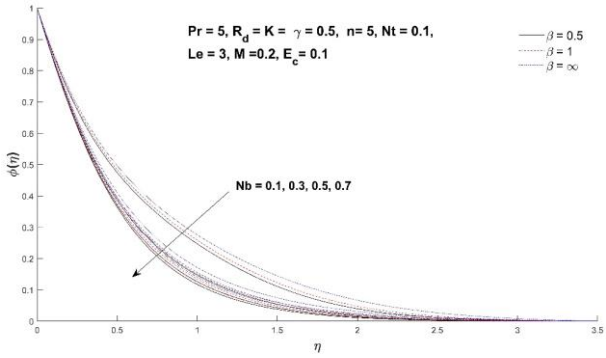

Figure 8: Influence of Nb on nanoparticle concentration for different values of β

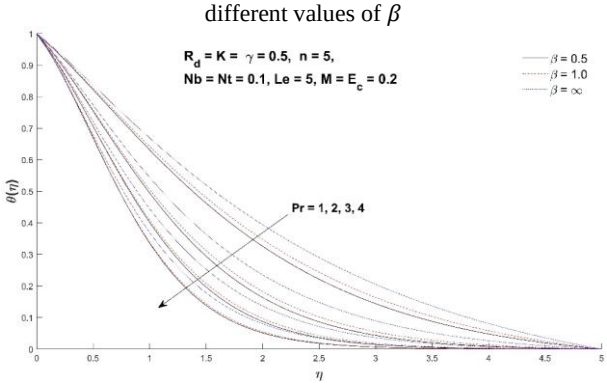

Figure 9: Influence of Pr on temperature profile for different values of β

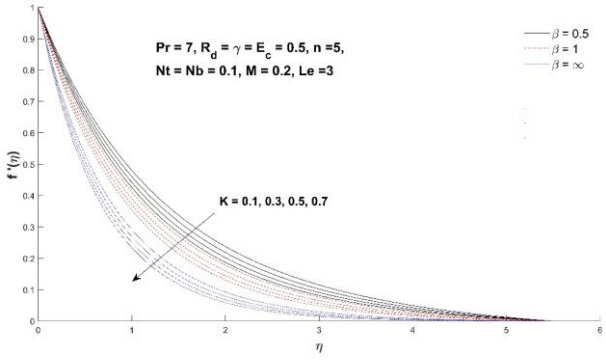

Figure 10: Influence of K on velocity profile for different values of β.

temperature increases but the nanoparticle concentration decreases as we increase the value of Nb. It is well known that as Nb increases, so does the random motion of nanoparticles, resulting in an increase in collisions with other nanoparticles. As a result, the kinetic energy is transformed into heat energy, and the temperature rises. But the rate of mass transfer decreases because of the tendency of the particle to get close to each other as Nb increases.

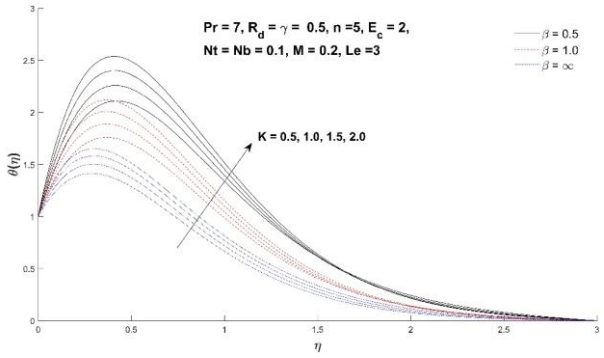

Figure 11: Influence of K on temperature profile for different values of β

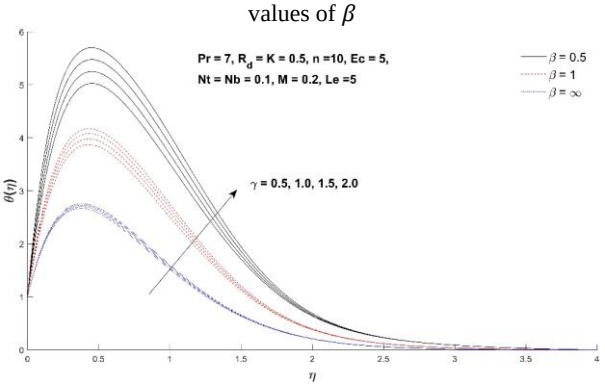

Figure 12: Influence of γ on temperature profile for different values of β

Figure (9) exhibit the effect of Pr on dimensionless temperature. Clearly temperature gets decrease as we increase the value of Pr. The main reason behind the fact that with the higher value in Pr the heat diffuses more rapidly that the momentum. It is also observed that at large Pr the temperature falls more drastically. The reason for the behavior is because the large values of Pr leads to the low thermal conductivity.

Figures (10) and (11) reveals the impact of K on both velocity and temperature profile for both Newtonian and non-Newtonian case. It is clear from the figure that with the increase in the value of K the velocity profile decreases but an opposite trend is seen in case of thermal boundary layer thickness.

The outcome of the chemical reaction parameter γ on temperature and nanoparticle concentration is depicted in fig. (12) and (13). It is clear from the graph that the boundary layer temperature increases but the concentration decreases as we increase the reaction parameter. It is very interesting to observe that the heat transfer rate of non-Newtonian fluid is quite larger than that of the Newtonian fluid as the reaction parameter varies.

The influence of Lewis number on temperature profile can be depicted in fig. (14). It is clear that the boundary layer warms up for very low values of Le. Fig. (15) shows the influence of radiation parameter on the temperature profile. It can be seen that the temperature increases with the increase in radiation parameter. This is

Table 2: Values of $-\theta'(0)$ and $-\phi'(0)$ for various values of β, M, Nt, Nb, Ec and γ when n=5, Le=Pr=2, Rd=1 and K=0.5

β	M	Nt	Nb	Ec	γ	$-\theta'(0)$	$-\phi'(0)$
0.5						0.1027	1.5473
1.0	0.5	0.1	0.1	0.5	0.5	0.1352	1.5027
1.5						0.1459	1.4835
	0.2					0.1027	1.5473
0.5	0.6	0.1	0.1	0.5	0.5	0.0719	1.5657
	1.0					0.00421	1.5838
		0.1				0.1027	1.5473
0.5	0.5	0.3	0.1	0.5	0.5	0.0742	1.9334
		0.5				0.0479	2.3705
			0.1			0.1027	1.5473
0.5	0.5	0.1	0.3	0.5	0.5	0.0637	1.4422
			0.5			0.0297	1.4203
				0.1		0.4317	1.3060
0.5	0.5	0.1	0.1	0.3	0.5	0.2674	1.4265
				0.5		0.1027	1.5473
					0.5	0.1027	1.5473
0.5	0.5	0.1	0.1	0.5	1.0	0.1025	1.8923
					1.5	0.1024	2.1693

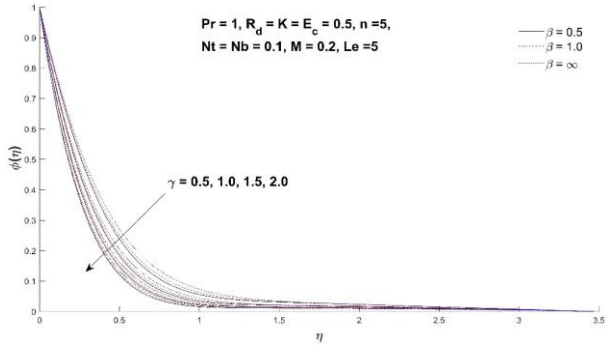

Figure 13: Influence of γ on nanoparticle concentration for different values of β

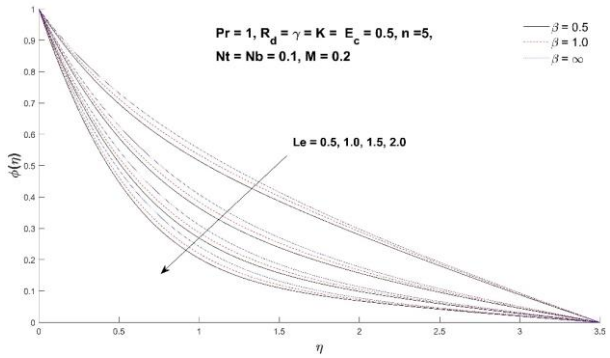

Figure 14: Influence of Le on nanoparticle concentration for different values of β

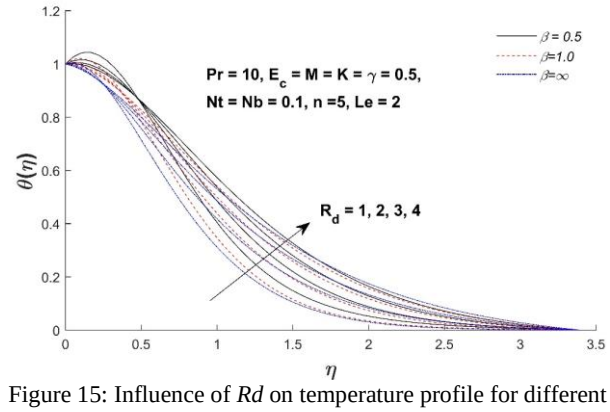

Figure 15: Influence of Rd on temperature profile for different values of β

due the fact that with the increase in Rd a heat energy is released to the fluid.

Keeping the other parameter preset, the effect of Casson parameter β, magnetic field parameter M, thermophoresis parameter Nt, Brownian motion parameter Nb , Eckert number Ec and chemical reaction parameter γ on the local Nusselt number and local Sherwood number are presented in Table 2. It is clear from the table that the Nusselt number decreases with the increase in Nt, M, Nb, Ec and γ but increases with the increase in β. On the other hand, the Sherwood number increases with the increase in Nt, M, Ec and γ but decreases in the case of Nb and β.

V. CONCLUSIONS

The numerical investigation of two-dimensional MHD Casson nanofluid flow over a non-linearly porous stretching sheet is presented in this article. The numerical results are successfully obtained by using MATLAB built-in software bvp4c. The findings are summarized as below-

- The velocity profile of the nanofluid declines with the increase in the value of Casson parameter, magnetic field parameter and porosity parameter.
- The thermal profile of the nanofluid escalates with the increase in magnetic field parameter, Brownian motion parameter, thermophoresis parameter, porosity parameter, chemical reaction parameter, Radiation Parameter.
- The temperature profile of the nanofluid decelerates with the increase in Prandtl number as well as Lewis number.
- Nanoparticle volume fraction in the boundary layer region enriches with the increase in the value of Thermophoresis parameter while it depletes with the increase in Brownian motion parameter and Chemical reaction parameter.
- Rate of heat transfer decreases with the increase in Brownian motion parameter, magnetic field parameter, thermophoresis parameter, Eckert number and

chemical reaction parameter but interestingly it increases with high Casson parameter.

- Mass transfer rate is found to increase by increasing the value of thermophoresis parameter, magnetic field parameter and Eckert number but it is noteworthy that it is found to decrease with the increase in Brownian motion parameter and Casson parameter.

REFERENCES

Abdal, S., Hussain, S., Siddique, I., Ahmadian, A. and Ferrara, M. (2021) On solution existence of MHD Casson nanofluid transportation across an extending cylinder through porous media and evaluation of priori bounds. *Scientific Reports*. **11**, 7799.

Abo-Dahab, S. M., Abdelhafez, M. A., Mebarek-Oudina, F. and Bilal, S. M. (2021) MHD Casson nanofluid flow over nonlinearly heated porous medium in presence of extending surface effect with suction/injection. *Indian Journal of Physics*. **95**, 2703–2717.

Brewster, M.Q. (1972) Thermal radiative transfer properties. *John Wiley* and *Sons*. New York.

Buongiorno, J. (2006) Convective transport in nanofluids. *Journal of Heat Transfer*. **128**, 240–250.

Cheng, C.Y. (2012) Free convection of non-Newtonian nanofluids about a vertical truncated cone in a porous medium. *International Communications in Heat* and *Mass Transfer*. **39**, 1348–1353.

Choi S.U.S. (1995) Enhancing thermal conductivity of fluids with nanoparticles. *ASME International Mechanical Engineering Congress* and *Exposition*. **66**, 99–105.

Divya, B.B., Manjunatha, G., Choudhari, R., Vaidya, H. and Prasad, K.V. (2021) Analysis of temperature dependent properties of a peristaltic MHD flow in a non-uniform channel: A Casson fluid model. *Ain Shams Engineering Journal.* **12**, 2181-2191.

Eastman, J. A., Choi, S.U.S., Li, S., Yu, W. and Thompson, L.J. (2001) Anomalously increased effective thermal conductivities of ethylene glycol-based nanofluids containing copper nanoparticles. *Applied Physics Letters*. **78**, 718–720.

Hady, F.M., Ibrahim, F.S., Abdel-Gaied, S.M. and Eid, M.R. (2011) Boundary-layer non-Newtonian flow over vertical plate in porous medium saturated with nanofluid. *Applied Mathematics* and *Mechanics (English Edition)*. **32**, 1577–1586.

Hayat, T., Muhammad, T., Shehzad, S.A. and Alsaedi, A. (2015) Three-dimensional boundary layer flow of Maxwell nanofluid: mathematical model. *Applied Mathematics* and *Mechanics (English Edition)*. **36**, 747–762.

Ibrahim, S.M., Lorenzini, G., Kumar, P.V. and Raju, C.S.K. (2017) Influence of chemical reaction and heat source on dissipative MHD mixed convection flow of a Casson nanofluid over a nonlinear permeable stretching sheet. *International Journal of Heat and Mass Transfer*. **111**, 346-355.

Jamshed, W., Uma Devi, S., Goodarzi, M., Prakash, M., Sooppy Nisar, K., Zakarya, M. and Abdel-Aty, A. H. (2021) Evaluating the unsteady Casson nanofluid over a stretching sheet with solar thermal radiation: An optimal case study. *Case Studies in Thermal Engineering*. **26**, 101160.

Joshi, N., Upreti, H., Pandey, A.K. and Kumar, M. (2021) Heat and Mass Transfer Assessment of Magnetic Hybrid Nanofluid Flow via Bidirectional Porous Surface with Volumetric Heat Generation. *Int. J. Appl. Comput. Math*. **7**(64).

Khan, W. A. and Pop, I. (2010) Boundary-layer flow of a nanofluid past a stretching sheet. *International Journal of Heat* and *Mass Transfer*. **53**, 2477–2483.

Kuznetsov, A.V. and Nield, D.A. (2010) Natural convective boundary-layer flow of a nanofluid past a vertical plate. *International Journal of Thermal Sciences.* **49**, 243–247.

Lee, S., Choi, S.U.S., Li, S. and Eastman, J.A. (1999) Measuring Thermal Conductivity of Fluids Containing Oxide Nanoparticles. *ASME. J. Heat Transfer.* **121**, 280–289.

Lund, L.A., Omar, Z., Khan, I., Sherif, E.S.M. and Abdo, H.S. (2020) Stability analysis of the magnetized Casson nanofluid propagating through an exponentially shrinking/stretching plate: Dual solutions. *Symmetry*. **12**,1162.

Mabood, F., Khan, W.A. and Ismail, A.I.M. (2015). MHD boundary layer flow and heat transfer of nanofluids over a nonlinear stretching sheet: A numerical study. *Journal of Magnetism* and *Magnetic Materials*. **374**, 569–576.

Makanda, G., Shaw, S. and Sibanda, P. (1999) Diffusion of Chemically Reactive Species in Casson Fluid Flow over an Unsteady Stretching Surface in Porous Medium in the Presence of a Magnetic Field. *Journals of Heat Transfer.* **121**, 280–289.

Makinde, O.D., Khan, Z.H., Ahmad, R. and Khan, W.A. (2018) Numerical study of unsteady hydromagnetic radiating fluid flow past a slippery stretching sheet embedded in a porous medium. *Physics of Fluids*. **30**, 083601.

Malik, M.Y., Salahuddin, T., Hussain, A. and Bilal, S. (2015) MHD flow of tangent hyperbolic fluid over a stretching cylinder: Using Keller box method. *Journal of Magnetism* and *Magnetic Materials*. **395**, 271–276.

Manjunatha, G., Choudhari, R., Prasad, K.V., Vaidya, H., Vajravelu, K. and Sreenadh, S. (2019) Peristaltic Pumping of a Casson Fluid in a Convectively Heated Porous Channel with Variable Fluid Properties. *Journal of Nanofluids*. **8**, 1446-1457.

Mukhopadhyay, S., Vajravelua, K. and Van Gorder, R.A. (2013) Casson fluid flow and heat transfer at an exponentially stretching permeable surface. *J. Appl. Mech.* **80**, 054502.

Mustafa, M., Hayat, T., Pop, I. and Aziz, A. (2011) Unsteady boundary layer flow of a Casson fluid due to an impulsively started moving flat plate. *Heat Transfer - Asian Research*. **40**, 563–576.

Nadeem, S., Mehmood, R. and Akbar, N.S. (2014). Optimized analytical solution for oblique flow of a Casson-nano fluid with convective boundary conditions. *International Journal of Thermal Sciences*. **78**, 90–100.

Nandy, S.K. (2013) Analytical Solution of MHD Stagnation-Point Flow and Heat Transfer of Casson Fluid over a Stretching Sheet with Partial Slip. *ISRN Thermodynamics*. **2013**, 108264.

Nield, D.A. and Kuznetsov, A.V. (2009) Thermal instability in a porous medium layer saturated by a nanofluid. *International Journal of Heat* and *Mass Transfer*. **52**, 5796–5801.

Oyelakin, I.S., Mondal, S. and Sibanda, P. (2016) Unsteady Casson nanofluid flow over a stretching sheet with thermal radiation, convective and slip boundary conditions. *Alex*and*ria Engineering Journal*. **55**, 1025-1035.

Pai, S.I., (1956) *Viscous Flow Theory*. Vol. 1. Laminar Flow, D. VanNostrand Co. New York, USA.

Pandey, A.K. and Kumar, M. (2017) Natural convection and thermal radiation influence on nanofluid flow over a stretching cylinder in a porous medium with viscous dissipation. *Alexandria Engineering Journal.* **56**, 55-62.

Pandey, A.K. and Upreti, H. (2021) Mixed convective flow of Ag–H2O magnetic nanofluid over a curved surface with volumetric heat generation and temperature dependent viscosity. *Heat Transfer*. **50**, 7251-7270.

Prasad, K. V., Vaidya, H., Choudhari, R., Khan S.U., Manjunatha, G. and Viharika, J.U. (2020) Slip flow of MHD Casson fluid in an inclined channel with variable transport properties. *Commun. Theor. Phys.* **72**, 095004.

Rafique, K., Anwar, M.I., Misiran, M., Khan, I., Alharbi, S.O., Thounthong, P. and Nisar, K.S. (2019) Numerical Solution of Casson Nanofluid Flow Over a Non-linear Inclined Surface with Soret and Dufour Effects by Keller-Box Method. *Frontiers in Physics*. **7**.

Raju, C.S.K., Sandeep, N. and Malvandi, A. (2016) Free convective heat and mass transfer of MHD non-Newtonian nanofluids over a cone in the presence of non-uniform heat source/sink. *Journal of Molecular Liquids*. **221**, 108–115.

Ramzan, M., Bilal, M., Chung, J.D. and Farooq, U. (2016). Mixed convective flow of Maxwell nanofluid past a porous vertical stretched surface – An optimal solution. *Results in Physics*. **6**, 1072–1079.

Rana, P., Bè, R. and Bég, O.A. (2012) Numerical solution for mixed convection boundary layer flow of a nanofluid along an inclined plate embedded in a porous medium. *Computers* and *Mathematics with Applications*. **64**, 2816–2832.

Rana, P. and Bhargava, R. (2012). Flow and heat transfer of a nanofluid over a non-linearly stretching sheet: A numerical study, *Communications in Nonlinear Science* and *Numerical Simulation*. **17**, 212-226.

Raptis, A. (1998) Radiation and free convection flow through a porous medium. *Int. Commun Heat Mass Transf.* **25**, 289–295.

Rashad, A.M., El-Hakiem, M.A. and Abdou, M.M.M. (2011) Natural convection boundary layer of a non-Newtonian fluid about a permeable vertical cone embedded in a porous medium saturated with a nanofluid. *Computers* and *Mathematics with Applications*. **62**, 3140–3151.

Schichting H. (1964). Boundary Layer Theory, *McGraw-Hill*. 6, New York.

Shashikumar, N.S., Archana, M., Prasannakumara, B.C., Gireesha, B.J. and Makinde, O.D. (2017) Effects of nonlinear thermal radiation and second order slip on Casson nanofluid flow between parallel plates. *Defect Diffusion Forum*. **377**, 84-94.

Singh, K., Pandey, A.K. and Kumar, M. (2021) Numerical solution of micropolar fluid flow via stretchable surface with chemical reaction and melting heat transfer using Keller-Box method. *Propulsion and Power Research*. **10**, 194-207.

Sparrow, E.M. and Cess, R.D. (1978) Radiation heat transfer. *Washington: Hemisphere*.

Upreti, H., Joshi, N., Pandey, A.K. and Rawat, S.K. (2021) Numerical solution for Sisko nanofluid flow through stretching surface in a Darcy–Forchheimer porous medium with thermal radiation. *Heat Transfer*. **50**, 6572- 6588.

Upreti, H., Pandey, A.K., Kumar, M. and Makinde, O.D. (2020) Ohmic Heating and Non-uniform Heat Source/Sink Roles on 3D Darcy–Forchheimer Flow of CNTs Nanofluids Over a Stretching Surface. *Arab. J. Sci. Eng.* **45**, 7705–7717.

Wang, X., Xu, X. and Choi, S.U.S. (1999) Thermal conductivity of nanoparticle-fluid mixture. *Journal of Thermophysics* and *Heat Transfer*. **13**, 474–480.

Xuan, Y. and Li, Q. (2003) Investigation on convective heat transfer and flow features of nanofluids. *Journal of Heat Transfer*. **125**, 151–155.

Zaib, A., Chamkha, A.J., Rashidi, M.M. and Bhattacharyya, K. (2018) Impact of nanoparticles on flow of a special non-Newtonian third-grade fluid over a porous heated shrinking sheet with nonlinear radiation. *Nonlinear Engineering*. **7**, 103-111.

Zhou, J.C., Abidi, A., Shi, Q.H., Khan, M.R., Rehman, A., Issakhov, A. and Galal, A.M. (2021) Unsteady radiative slip flow of MHD Casson fluid over a permeable stretched surface subject to a non-uniform heat source. *Case Studies in Thermal Engineering*. 26.

Received: December 23, 2021
Sent to Subject Editor: December 23, 2021
Accepted: June 26, 2022
Recommended by Subject Editor Gianfranco Caruso